

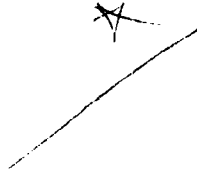
MICROCOPY RESOLUTION TEST CHART
NATIONAL BUREAU OF STANDARDS-1963-A

AD-A161 041

REPORT DOCUMENTATION PAGE				
1a. REPORT SECURITY CLASSIFICATION UNCLASSIFIED		1b. RESTRICTIVE MARKINGS		
2a. SECURITY CLASSIFICATION AUTHORITY		3. DISTRIBUTION / AVAILABILITY OF REPORT		
2b. DECLASSIFICATION / DOWNGRADING SCHEDULE		Approved for public release; distribution unlimited.		
4. PERFORMING ORGANIZATION REPORT NUMBER(S) NRL Memorandum Report 5677		5. MONITORING ORGANIZATION REPORT NUMBER(S)		
6a. NAME OF PERFORMING ORGANIZATION Naval Research Laboratory	6b. OFFICE SYMBOL (if applicable) Code 4180.2	7a. NAME OF MONITORING ORGANIZATION		
6c. ADDRESS (City, State, and ZIP Code) Washington, DC 20375-5000		7b. ADDRESS (City, State, and ZIP Code)		
8a. NAME OF FUNDING / SPONSORING ORGANIZATION	8b. OFFICE SYMBOL (if applicable)	9. PROCUREMENT INSTRUMENT IDENTIFICATION NUMBER		
8c. ADDRESS (City, State, and ZIP Code)		10. SOURCE OF FUNDING NUMBERS		
		PROGRAM ELEMENT NO.	PROJECT NO.	TASK NO.
				WORK UNIT ACCESSION NO. DN280-477
11. TITLE (Include Security Classification) Sounder-Updated Statistical Model Predictions of Maximum Usable Frequency for HF Sky Wave Propagation				
12. PERSONAL AUTHOR(S) Reilly, M.H. and Daehler, M.				
13a. TYPE OF REPORT Interim	13b. TIME COVERED FROM _____ TO _____	14. DATE OF REPORT (Year, Month, Day) 1985 October 30	15. PAGE COUNT 25	
16. SUPPLEMENTARY NOTATION				
17. COSATI CODES			18. SUBJECT TERMS (Continue on reverse if necessary and identify by block number)	
FIELD	GROUP	SUB-GROUP	HF predictions	
			Sounder updates	
19. ABSTRACT (Continue on reverse if necessary and identify by block number)				
<p>Measured solar parameters, such as sunspot number or 10.7 cm flux, have traditionally been used as inputs to drive statistical model predictions of maximum usable frequencies (MUFs) on HF radio sky wave paths of interest. Much greater accuracy can be obtained by using ionospheric sounder inputs to drive or "update" statistical model predictions, and this is demonstrated here using oblique-incidence sounder data from the DoD Solid Shield exercises on May 12-14, 1981. From analysis of ionograms collected for several paths every fifteen minutes, it is found that deployment of a reasonable number of sounders in a large area, in order to update the simple statistical model, MINIMUF, yields MUF prediction capability on unsounded communication paths in the area within 0.4 MHz rms error. This value is obtained from real-time updating and a spatial interpolation process developed here, whereby data at sounder control points is interpolated to ionospheric reflection points for communication paths of interest. The results from the interpolation are found to be at least 20-30% more accurate than updating at any one of the nearby sounder control points. The updating procedure applies under day and night conditions,</p> <p style="text-align: right;">(Continues)</p>				
20. DISTRIBUTION / AVAILABILITY OF ABSTRACT <input checked="" type="checkbox"/> UNCLASSIFIED/UNLIMITED <input type="checkbox"/> SAME AS RPT <input type="checkbox"/> DTIC USERS		21. ABSTRACT SECURITY CLASSIFICATION UNCLASSIFIED		
22a. NAME OF RESPONSIBLE INDIVIDUAL M. H. Reilly		22b. TELEPHONE (Include Area Code) (202) 767-2891	22c. OFFICE SYMBOL Code 4180.2	

19. ABSTRACT (Continued)

and also works well in a forecasting mode (not real-time), where it is found to work better in this case than a statistical trend line approach for daytime forecasting.



SOUNDER-UPDATED STATISTICAL MODEL PREDICTIONS OF MAXIMUM USABLE FREQUENCY FOR HF SKY WAVE PREDICTIONS

INTRODUCTION

A program for accurate prediction of the maximum usable frequency (MUF) for HF sky wave propagation on any set of transmitter-ionosphere-receiver circuits would be invaluable to HF system planners and frequency managers. A frequency in the FOT (frequencies of optimum transmission) band, slightly below the MUF, could then also be accurately predicted. With this capability to track FOT variations accurately, it becomes more worthwhile to consider the pooling of available HF frequency resources and the coordinated assignment of frequencies to particular users based on the MUF and FOT predictions. The success rate for communications should be significantly enhanced. This paper evaluates the relative merits of various techniques for improvement of MUF predictions based on the use of a sounder-updated statistical model.

The statistical model used here is MINIMUMUF [Rose, Martin, and Levine, 1978; Rose and Martin, 1978; Sailors, Moision, and Brown, 1981; Sailors, 1984], which is a relatively simple semiempirical MUF prediction model based on several thousand maximum observed frequencies (MOFs) collected between 1960 and 1976 on 23 different paths. Despite its simplicity, it tests comparably well with more complex MUF prediction models. A MUF prediction on a given path is generated from the input of transmitter and receiver coordinates, the time, and the sunspot number or 10.7 cm solar radio flux for the day. When the model was tested against 4668 MOFs measured on 25 paths, it produced an rms error of 3.71 MHz [Rose et al, 1978; Sailors et al, 1981]. This compares well with the predictions of large-scale codes with similar inputs. MINIMUMUF is the software module used to predict MUF values in CLASSIC PROPHET and ADVANCED PROPHET (APES) systems [Sailors, 1984].

Later investigations [Uffelman, 1981; Uffelman and Harnish, 1981,1982; Uffelman and Hoover, 1984; Uffelman, Harnish, and Goodman, 1984; Daehler, 1984] have shown that MUF predictions could be significantly improved by locating an ionospheric oblique-incidence sounder in the general vicinity of

circuits for which MUF predictions are desired, and then using sounder data, instead of the measured sunspot number or 10.7 cm solar radio flux, to drive the statistical model predictions. This capability for sounder-updating of MINIMUF has recently been incorporated into the APES system [Sailors, 1984]. The updating procedure consists of forcing MINIMUF to fit the sounder MUF value at a given time by defining an effective or pseudo-sunspot number (or pseudo-flux) for this purpose, and then using it to drive the MUF predictions on the various circuits. Previous studies have shown an advantage from sounder-updating once or a few times a day, and have indicated further improvement in accuracy to be gained from updating more frequently [Uffelman and Harnish, 1982]. This is further investigated in the next section.

If the use of one sounder for updating purposes gives an advantage, it is of interest to know what additional accuracy can be obtained by deploying more sounders in a communications area. This is also investigated in the next section. The general approach would be to use sounder data to characterize the ionosphere at various locations, i.e., "sounder control points", and then interpolate the information at these points to the control points for the unsounded HF circuits of interest. It will be shown how this updating method is coupled to MINIMUF predictions for these circuits, and how accurate it is relative to previous methods.

An opportunity to develop and test updating methods is provided by the sounder data taken during the DoD Solid Shield exercises during May 1981. The configuration of oblique-incidence sounders used is shown in Figure 1. Sounder transmitter locations are shown by the hexagons, and the receiver positions are indicated by squares. The sounder paths are shown by the solid lines. Also shown are triangles which locate the midpoints of the various sounder paths. These are taken to be the sounder control points (SCPs) for the propagation modes involving one ionospheric reflection, and the MUF values for these one-hop ionogram modes comprise the data set of interest for this study. The ionogram is a plot of time-of-transit of a pulse on a propagation path vs the wave frequency. The ionogram retardation effects in the one-hop modes may be expected to characterize the ionosphere near midpath, since this is where most of the refraction and retardation occur, and previous studies [Basler and Scott, 1973; Reilly, 1985a, 1985b] have confirmed this expectation. Hence, the ionosphere is sensed at the SCP positions in Figure 1. Of particular interest for this study are those five positions east of 80°W longitude, for which a nearly complete set of MUF data for F-layer

reflections has been collected every fifteen minutes during May 12-14. It is seen from Figure 1 that the SCP for the Shaw-Norfolk path is interior to two different triangles of SCPs, one triangle being obtained from the other by replacing the Lejeune-Norfolk SCP by the MacDill-Norfolk SCP. The other SCPs common to both triangles are associated with the Shaw-Bragg and Driver-Bragg paths. Sounder-updated MINIMUMF predictions will be made for the interior SCP and compared to measured MUF values for this point. Updating will be done at each of the SCPs at the triangle vertex points (i.e., along the path associated with the SCP). Interpolated data for these triangles of points will also be used for MUF predictions at the interior point.

Another technique which is tested below is related to temporal perishability of sounder-updated MINIMUMF predictions. It has been found in previous work (Uffelman et al, op.cit.) that, because pseudo-sunspot number for an SCP varies with time, the advantage gained from sounder-updating tends to vanish for lag times between the sounder measurement and the MUF prediction in excess of three or four hours. In order to improve MUF predictions at future times, an attempt has been made to exploit the fact that ionospheric parameters, such as foF2, tend to show a noisy variation in their daytime dependence about a fairly well-defined background dependence [Reilly and Yamamura, 1984; Reilly, 1985b]. In particular, when foF2² is plotted against the cosine of the effective solar zenith angle, this background dependence appears nearly linear. Hence, it appears possible to average sounder data over a, e.g., two hour period in a linear regression analysis to establish the trend line parameters for foF2², and then use this trend line in conjunction with MINIMUMF for predictions of MUF into the future. This is another of the techniques which are tested and evaluated relative to each other in the following analysis.

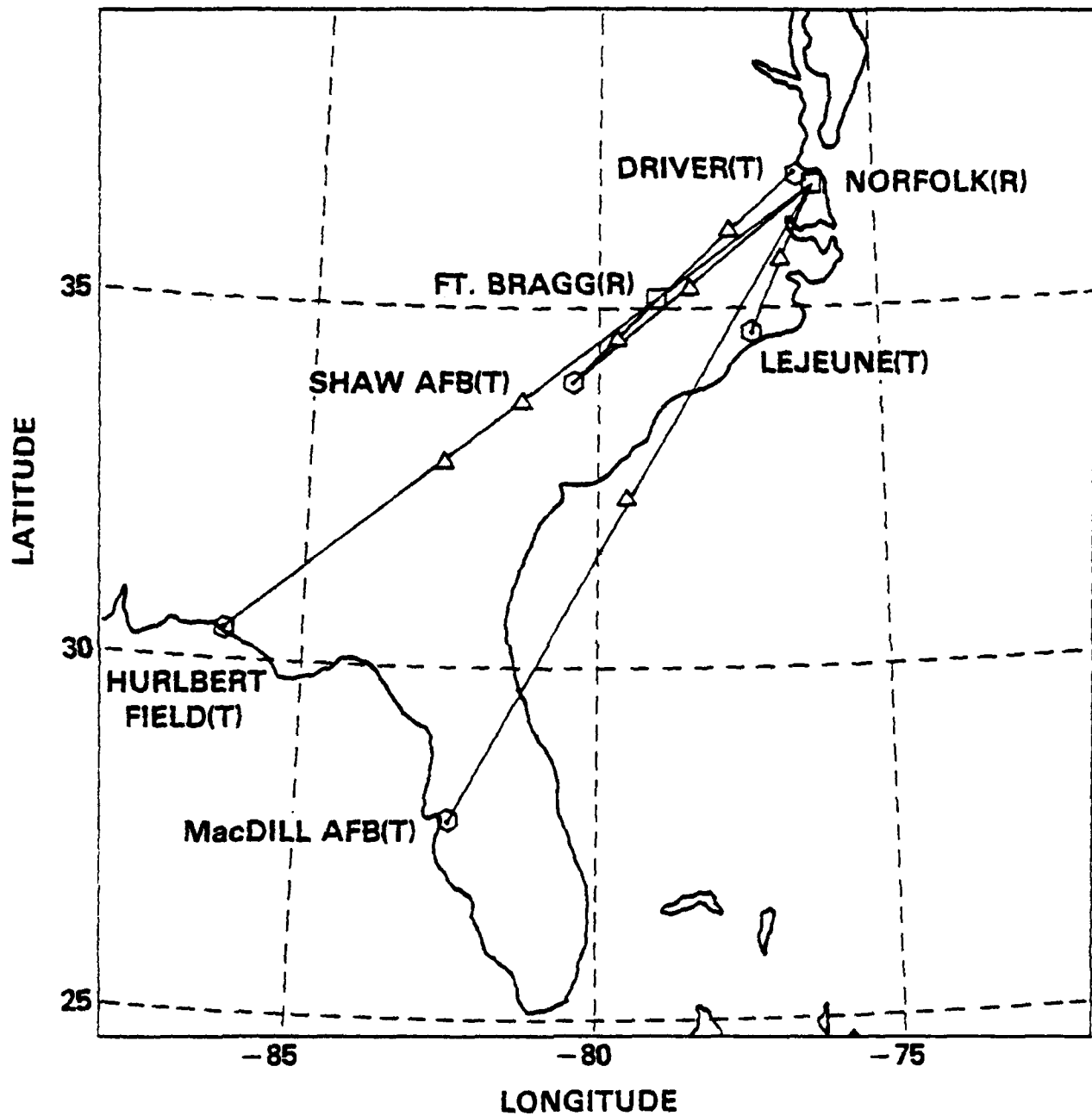


Fig. 1 Configuration of oblique-incidence sounders used in the DoD Solid Shield exercises.

UPDATING TECHNIQUES AND RESULTS

In this section MUFs measured on the 489 km Shaw-Norfolk Path in Figure 1 will be compared with updated MINIMUMF predictions. A standard MINIMUMF application, which uses the daily measured 10.7 cm solar flux reported by World Data Center A for MUF predictions, will be compared with the various sounder-updated MINIMUMF predictions mentioned above. The relative merits of these techniques will thus be discerned, first for real-time predictions, in which sounder measurements keep pace with MUF predictions on the unsounded path, and then for near-real-time predictions in which sounder measurement times can lag the prediction time by some number of hours.

For convenience, some of the equations from MINIMUMF [Rose, Martin, and Levine, 1978] are repeated here in a suitable form. The predicted MUF (in MHz) is given as

$$\text{MUF} = (\text{foF2}) (M) \quad (1)$$

where the M-factor includes a dependence on the range of the path, and foF2 is the maximum plasma frequency of the F-layer at the SCP for the path. The model ionosphere in MINIMUMF is a parabolic F-layer which rises from zero plasma frequency at an altitude 209 km up to its maximum at 290 km. Hence, a large weight of empirical data is lumped into foF2, which is given as

$$\text{foF2} = f(R) (A_0 + A_1 [\cos \chi_{\text{eff}}]^{1/2})^{1/2} \quad (2)$$

where $f(R)$ is a function dependent on the sunspot number R , A_0 and A_1 are positive constants, and χ_{eff} is the effective solar zenith angle. The latter is related to the actual solar zenith angle χ between the overhead direction and the solar direction at an F-layer height by

$$\tau \frac{d}{dt} (\cos \chi_{\text{eff}}) + \cos \chi_{\text{eff}} = \cos \chi \quad (3)$$

The effect of τ is to cause a time delay between the solar perturbation and the ionospheric response. In particular, foF2 in (2) reaches a maximum at a time Δt_{max} later than local noon. It is straightforward to compute the

dependence of this shift on τ , and this is shown in Figure 2. Times shown are in units of duration of ionospheric daylight, i.e., the time interval during which $\cos \chi > 0$. For example, $\Delta t_{\max} = 0.1$ corresponds to 1.6 hrs. when the daylight duration is 16 hrs. For values of τ up to a few hours, Δt_{\max} and τ are essentially the same.

The value of $f(R)$ in (2) is defined by the updating procedure, but for specificity in defining an effective 10.7 cm flux, the sunspot number dependence is taken from MINIMUF-3.5 [Rose et al, 1978], in which $A_0 = 6$, $A_1 = 58$,

$$f(R) = 1 + (R/250) \quad , \quad (4)$$

and sunspot number R is related to 10.7 cm flux F by

$$R = \{ [0.52998 - 0.00356(63.75 - F)]^{1/2} - 0.728 \} / 0.00178 \quad (5)$$

This expression is easily inverted to find F in terms of R .

The procedure employed here for sounder-updating is to input the MUF values for each sounder path and determine from (1)-(5) and the rest of the MINIMUF algorithm the corresponding values of effective flux F for the associated SCP. The input and output parameters for the time period of interest are shown for the interior SCP (Shaw-Norfolk in Figure 1) in Figure 3. Input MUF data start at 15.85 hrs. (UT) on May 12 and end at 23.85 hrs. on May 14. Also shown by the arrows in the right-hand margin of Figure 3 are the measured 10.7 cm flux values [Coffey, 1981] for the three days involved. The difference between measured fluxes and effective fluxes, as determined from MINIMUF and the MUF values measured every fifteen minutes, suggests the advantage to be gained from sounder updating. The daytime values of MUF on May 12 and 13 are close to each other, but the May 14 values are relatively depressed, which is a characteristic ionospheric response to geomagnetic storms. The pronounced diurnal variation of the effective flux in Figure 3 is not taken into account by the use of a single measured flux for the day. It appears that MUF predictions for a set of times on a given day would be better obtained from the use of the effective fluxes at the corresponding times on the preceding day.

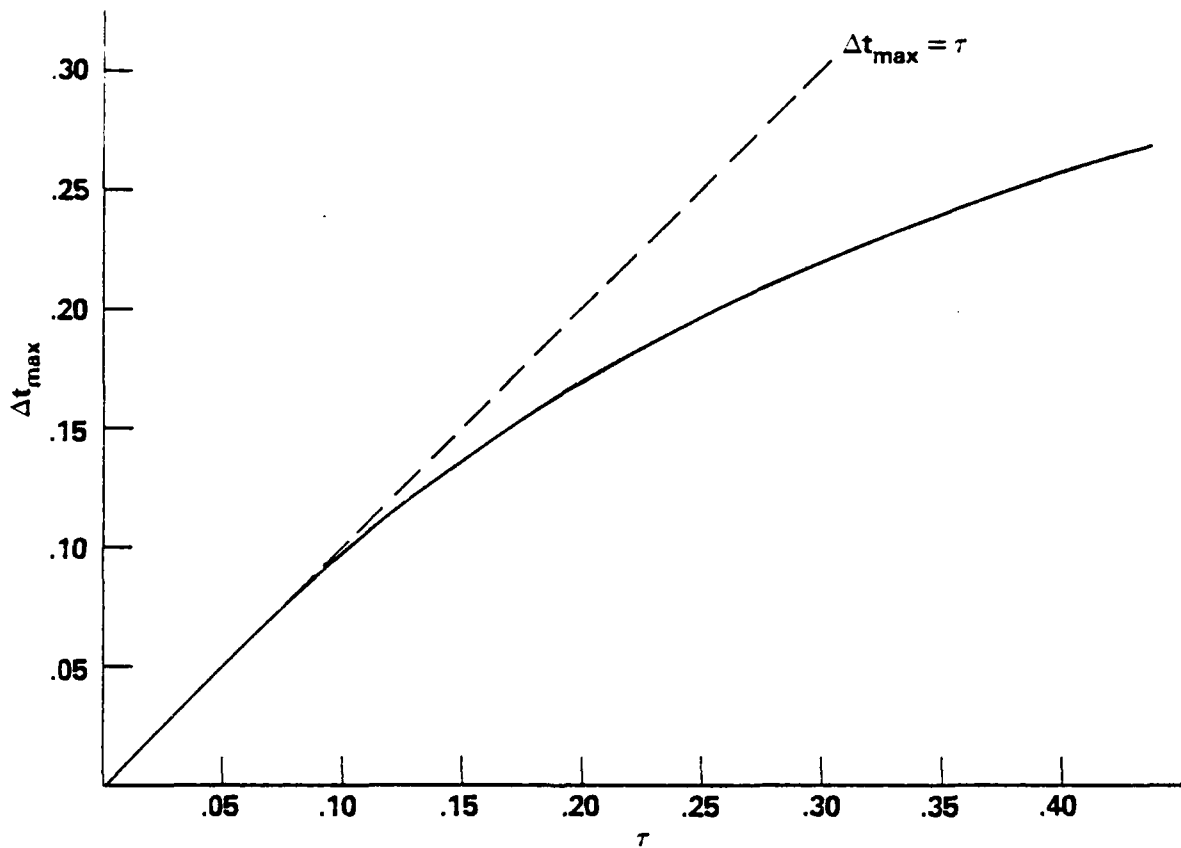


Fig. 2 Time shift Δt_{\max} from local noon for maximum F-layer density in the MINIMUF model as a function of decay time τ for the effective solar zenith angle. Time is measured in units of the daytime duration $T_{\text{sunset}} - T_{\text{dawn}}$.

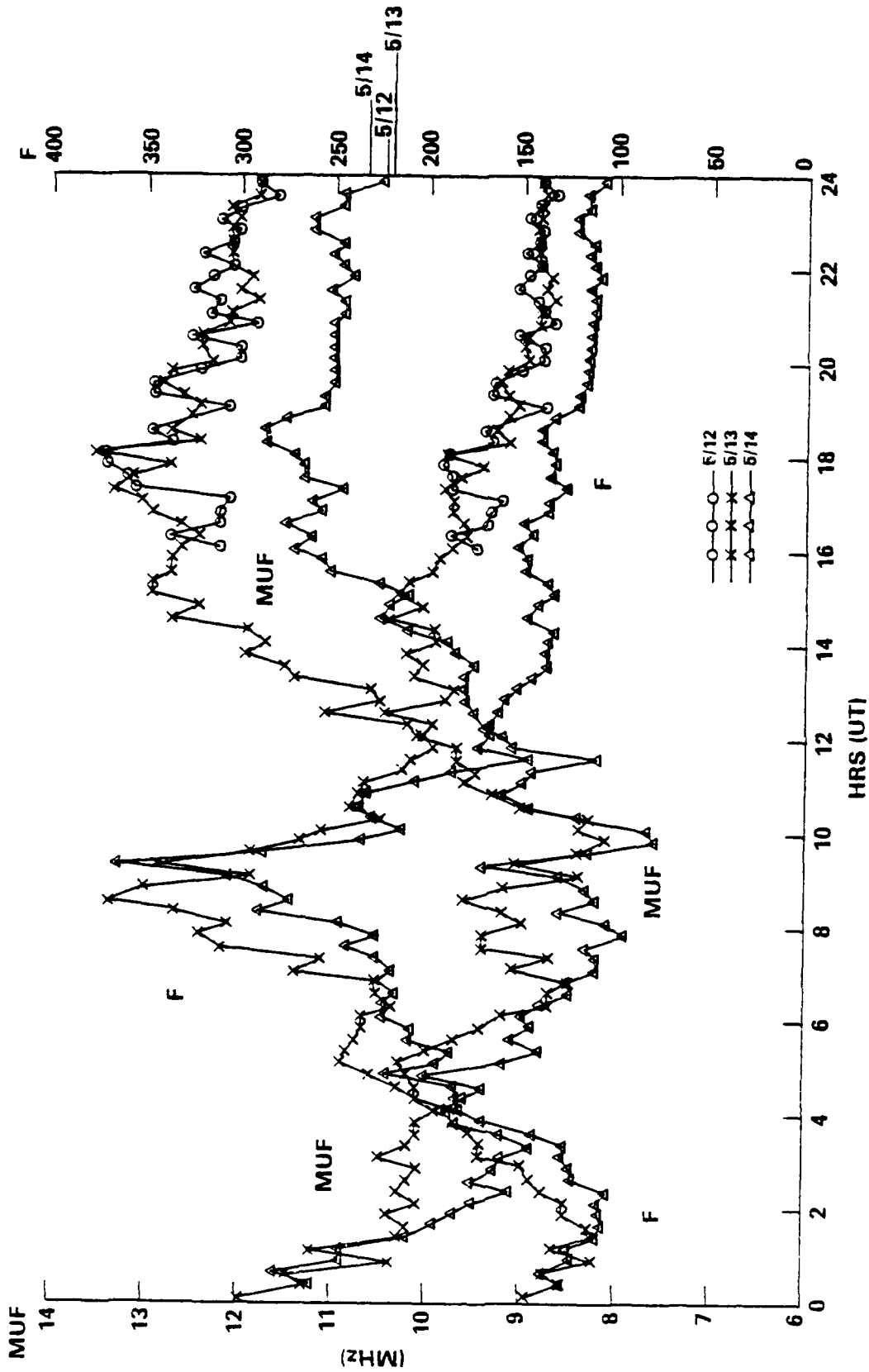


Fig. 3 MUF and effective 10.7 cm flux F data for SCP4 in the time period considered. Units of F are $10^{-22} \text{ Wm}^{-2} \text{ Hz}^{-1}$. The measured daily values of F are shown by arrows in the right-hand margin.

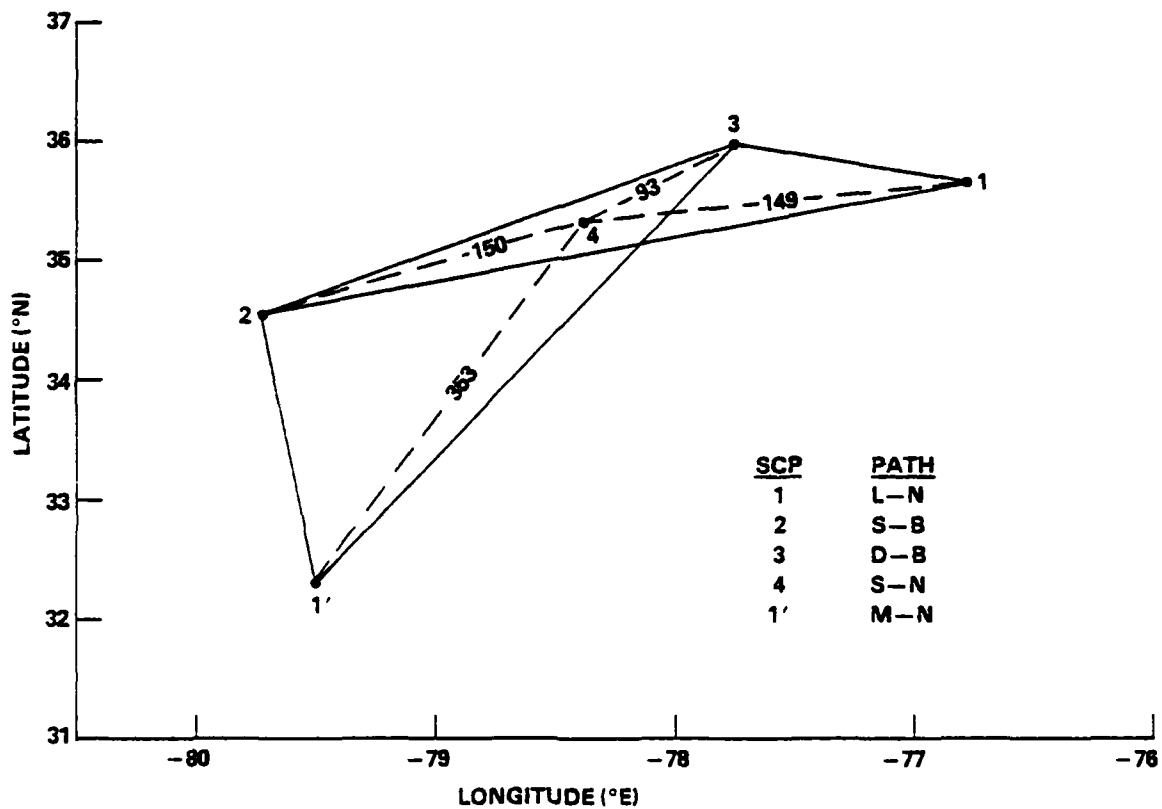


Fig. 4 Two sounder control point triangles used for MUF predictions at SCP4. Ranges (in km.) from SCP4 to the various triangle points are written along the dashed lines.

As stated previously, various updating techniques are to be tested on the data for May 12-14 with respect to two triangular configurations in Figure 1, which are shown in greater detail in Figure 4. With the SCP numbering convention shown, the triangles are $\Delta 123$ and $\Delta 1'23$. The correspondence of the SCPs to the paths in Figure 1 is also tabulated (e.g., L-N corresponds to the Lejeune-Norfolk path). Both triangles share the same interior point SCP4. Updating will be performed with the three vertex points of each triangle to predict the MUF at SCP4. This value will be compared with the measured MUF at this interior point, and an rms error E for the prediction will be extracted, i.e.,

$$E^2 = \frac{1}{N} \sum_{i=1}^N [MUF_i(\text{pred.}) - MUF_i(\text{meas.})]^2, \quad (6)$$

where i runs over the N data points in Figure 3 for the time period of interest. A comparison of E values for the various updating techniques will test their relative merit. MUF values were found from the ionograms measured for each sounder path every fifteen minutes, but the measurement times were different for different sounders. All sounder MUF values were transformed to the measurement times for the interior point through simple linear interpolation, and these transformed values were used for the calculations of E . Also shown in Figure 4 are dashed lines from the interior point to each of the vertex points of the triangles. The numbers along each of these dashed lines give the distance in km from the interior point to the corresponding vertex point.

Values of E in (6) can, as in previous work, be obtained by updating MINIMUMUF at each SCP triangle vertex point in Figure 4. In this process the effective fluxes determined from MUF values for the particular SCP are used in conjunction with MINIMUMUF to predict the MUF for the interior point. A new updating technique is to spatially interpolate the effective fluxes for the three SCP triangle vertex points to the interior point location. If the effective fluxes for the triangle vertex points at a given time are denoted by F_i (i runs from 1 to 3 or 1' to 3 in Figure 4), the interpolated effective flux for the interior point F can be written as a weighted average of the F_i :

$$F = \sum_i w_i F_i, \quad (7)$$

where the three weighting factors w_i depend only on the SCP and interior point locations, and they add up to unity. For a linear dependence on latitude (L) and longitude (l) as the interpolation scheme, it is found for $\Delta 123$ that

$$w_i = [(\ell_j - \ell_k)L + (L_k - L_j)\ell + d_{jk}] / [d_{12} + d_{23} + d_{31}] \quad , \quad (8)$$

where

$$d_{rs} \equiv L_r \ell_s - L_s \ell_r \quad , \quad (9)$$

and i, j , and k in (8) refer to a cyclic permutation of the indices 1, 2, and 3. Here, L and l are the latitude and longitude of the interior point. For the other triangle, l is replaced by l' . Note that this interpolation formula is indeed linear, that $w_i = 1$ when the interior point coincides with SCP_i , and that $w_i = 0$ when the interior point coincides with SCP_j or SCP_k , as required.

When real-time (no time lag between the effective flux determination and the MUF prediction at the interior point) updating is employed with the techniques of the preceding paragraph to predict MUFs at SCP_4 , the results of Table 1 are found. The first four rows are obtained from SCP effective flux determinations every fifteen minutes during May 12-14, except for a few MUF values which were missing from the data set. The time interval spanned for $\Delta 1234$ was 15.85 hrs (UT) on May 12 to 23.85 hrs on May 14. Because MUF values were not available for SCP_1' in Figure 4 after 16.6 hrs on May 14, this was the upper time limit for $\Delta 1'234$. The last row of the table was for the daily measured 10.7 cm flux inputs [Coffey, 1981] shown by the arrows in the right-hand margin of Figure 3, i.e., $F = 223.4$ on May 12, 221.3 on May 13, and 232.5 on May 14. The numbers in this row are large, compared to the rms errors for the effective flux inputs in the first four rows of the table. This shows the advantage to be gained from frequent sounder updating of the statistical model. The numbers for each triangle in the second, third, and fifth rows of Table 1 would be the same, if it were not for the additional eight hours of data processed for $\Delta 123$ on May 14. Of particular note in Table 1 is a significant increase in accuracy obtained from spatial interpolation of effective fluxes from the SCP triangle vertex points. This approach, with its high accuracy, can be valuable in a frequency management system which involves the deployment of an ionospheric sounder network. This

will result in an SCP grid which covers an area of interest. For a given communication circuit, with its associated midpath point, an SCP triangle which surrounds this point, presumably the smallest one possible, may be identified for spatial interpolation purposes. If this SCP triangle cannot be identified, data from the closest SCP could be used for updating.

While the preceding results have used a linear interpolation scheme, this is not necessarily the optimum choice. Evaluation of the weighting coefficients of the linear scheme in (8) and (9) for SCP4 in Figure 4 gives for the two triangles:

$$\begin{aligned} w_1 &= 0.190, w_2 = 0.414, w_3 = 0.396 && (\Delta 123) \\ w_{1'} &= 0.080, w_2 = 0.251, w_3 = 0.669 && (\Delta 1'23) \end{aligned}$$

The values for $\Delta 123$ run counter to the notion that the weighting coefficient for each SCP should vary inversely as the distance of that SCP from the interior point. In particular, SCP3 is weighted slightly less than SCP2, even though SCP2 is 61% further from the interior point in Figure 4 than SCP3, and SCP1 is weighted substantially less than SCP2, even though they are nearly equidistant from the interior point. Accordingly, an interpolation scheme has been tried in which the weighting factor for SCP_i depends on the range D from this point to SCP4, the interior point, according to an exponential range decay law:

$$w_i = \exp(-D_{i4}/\alpha) / \sum_j \exp(-D_{j4}/\alpha) \quad , \quad (10)$$

where the denominator simply normalizes the weighting coefficient. The results are shown in Table 2. The first row of the table involves the use of $\alpha=70$ km in (10), which approximately minimizes the associated value of E for $\Delta 123$ (as a function of α). This minimum E (0.35MHz) is only slightly less than the linear interpolation entry for $\Delta 123$ in Table 1. The second row of Table 2 involves $\alpha=400$ km in (10), which approximately minimizes the associated value of E for $\Delta 1'23$, and this minimum value is less than the linear interpolation entry for $\Delta 1'23$ in Table 1. There is, however, no single value of α which gives E values less than both interpolation values in Table 1. Hence, these results do not specifically indicate that one interpolation scheme is fundamentally preferable to the other. Another

interpolation scheme was tried in which the exponents in (10) were squared, which might be termed Gaussian range decay, but the results for this case were very similar to the results for exponential range decay in (10). From an operational point of view it may be preferable to adopt a weighting law like (10) and assign a value of α to each of the various possible SCP triangles, as determined from pre-testing of the type discussed here.

TABLE 1

RMS errors for real-time MUF predictions at SCP 4 for May 12-14 using updated MINIMUF with various 10.7 cm radio flux inputs.

<u>Flux Used For Updating</u>	<u>E (MHz) for $\Delta 123$</u>	<u>E (MHz) for $\Delta 1'23$</u>
Eff. at 1 or 1'	0.98	0.80
Eff. at 2	0.52	0.51
Eff. at 3	0.57	0.59
Interpolated Eff.	0.37	0.40
Daily Measured	2.46	2.12

TABLE 2

RMS errors for real-time MUF predictions at SCP 4 for May 12-14 using a flux-interpolation scheme with exponential range decay weighting.

<u>Decay Length α (km.)</u>	<u>E (MHz) for $\Delta 123$</u>	<u>E (MHz) for $\Delta 1'23$</u>
70	0.35	0.43
400	0.41	0.35

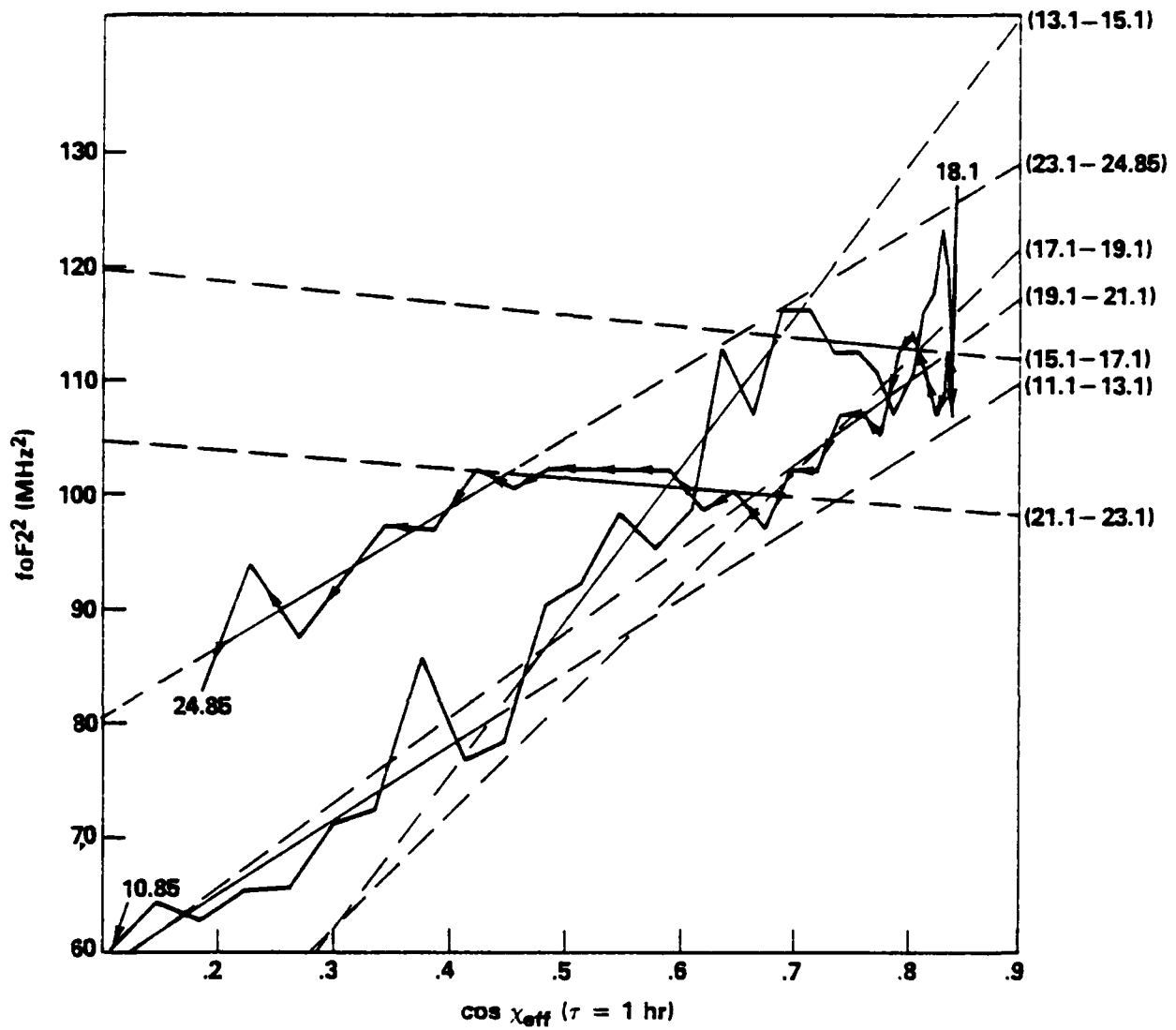


Fig. 5 Variation of daytime $foF2^2$ values (heavy jagged lines) for SCP4 on May 13 from MINIMUF with $\tau=1$ hour. Trend lines are the lighter, partially dashed lines determined during time intervals listed in the right-hand margin.

So far, the discussion has centered on real-time updating, in which there is no appreciable time delay between measurements and predictions. The case of finite delay between measurements and predictions is also of interest. One technique is to simply employ the latest interpolated effective flux determination for future predictions. Another technique may be based on the use of a statistical trend line for predictions [Reilly, 1984,1985b]. In this case, foF2 values are determined from the observed MUF values from (1) and the M-factor model of MINIMUF. A plot of foF2² vs cosχ_{eff}, where the latter is also determined from MINIMUF, then appears as shown by the dots connected by the heavy line segments in Figure 5. Also seen are light dashed lines which will be temporarily ignored. Figure 5 shows the variation at SCP4 for May 13 during daylight hours. Starting at 10.85 hrs (UT), foF2² shows a noisy variation about a roughly linear background dependence on cosχ_{eff} up to a maximum near 18.1 hrs (UT). This is about one hour past local noon (minimum actual solar zenith angle). After this time the noisy variation of foF2² decreases with cosχ_{eff} through a transition region into a more nearly linear background dependence in the late afternoon hours. This near-linear background dependence in the morning and late afternoon hours suggests the use of trend lines on these variables for predictions. In order to enhance this linearity, the value of τ in (3) has been forced to be one hour in the MINIMUF algorithm, in accordance with observations for all the sounders involved during May 12-13 that the MUF values reach their maximum values around 18 hrs (UT), one hour past local noon (cf. Figure 3). The previous results (Tables 1 and 2) have let MINIMUF determine the τ value, as per usual, which is calculated to be about 6.4 hrs in this case. This would imply a maximum value of cosχ_{eff} from Figure 2 at a little past 21 hrs (UT). The trend line approach tested here for a given MUF prediction time and delay time is to process the eight MUF values for each SCP which include and precede the prediction time minus the delay time. In particular, the process is a linear regression analysis to determine the constants A and B in

$$\text{fof2}^2 = A + B \cos\chi_{\text{eff}} \quad (11)$$

Eight fof2² values have been used, in order to average out noise variations. Hence, the A and B values are supposed to describe the linear background dependence, and this is to be used for future predictions. Results of this procedure are shown in Figure 5 by the lighter lines which show trend lines

for various two-hour intervals, labelled in the right-hand margin. Each trend line is solid in the interval for which it was determined and dashed outside this interval. Because of the wide slope variations in some of the trend lines, it is expected that each trend line could be useful for short-term excursions into the future, but that long-term prediction would be poor. For example, it is inadvisable to use a morning trend-line for predictions at an afternoon time.

The preceding trend line approach for daytime predictions is tested against the effective flux approach, previously discussed, for various delay times in Table 3. The predictive results for a sounded path are given for SCP4 by the first two rows of numbers, and linear triangular interpolation is used to predict at SCP4 from the sounder results at the triangle vertex points in the subsequent rows of Table 3. In the effective flux approach the interpolation is on the SCP fluxes at the prediction time minus the delay time. In the trend line approach the interpolation is on the A and B coefficients separately, in conjunction with the value of $\cos\chi_{\text{eff}}$ for the interior point at the prediction time in (11). The results show that the effective flux approach gives consistently better predictions in this case than the trend line approach, although only slightly better for the smaller time delays in Table 3. In order to obtain a better understanding of this, calculations were also performed by taking the foF2² values in the two-hour interval used for the trend line approach and finding a simple average of their values for the predictions. This corresponds to forcing B=0 in (11). The trend line approach (B≠0) consistently gave better results (smaller rms errors) for small time delays than the B=0 results. As the number averaged in the B=0 approach decreased from eight to one, the results approach the effective flux results; the trend line approach tended to get worse. Hence, when the noise variations are averaged out, the trend line approach is superior for predictions than the corresponding B=0 case for small time delays when the time interval for averaging exceeds one hour. The reverse is true when the time delays begin to exceed one hour or so. The effective flux results, which are consistently superior, apparently enjoy an advantage from including the noise variations. This noise is thought to arise principally from travelling ionospheric disturbances, which often simultaneously affect both the control point of interest (the interior point here) and nearby SCPs, such as in this study. In this case it is plausible that the inclusion of noise variations in the effective flux approach offers an advantage for

predictions. In the use of larger triangles for interpolation, in which noise variations between the various control points is less correlated, it may yet turn out that the trend line approach gives somewhat better prediction accuracy for small time delays. The effective flux approach discussed above now seems to be the method of choice, however, particularly because of its accuracy, simplicity, and applicability to both daytime and nighttime predictions. Use of the spatial interpolation scheme is found to enhance the accuracy of near-real-time updating, as compared to updating at a single SCP, similarly to the results of Table 1.

TABLE 3

RMS errors for MUF predictions at SCP 4 during daytime hours, May 12-14, for various time delays between measurements and predictions. MINIMUMUF is updated by measurements at SCP4 or by linear interpolation of data at SCP triangle vertex points. Predictions are based on the effective flux (EF) or trend line (TL) methods.

Description	Time Delays (hrs)				
	0.	0.5	1.0	1.5	2.0
EF at SCP4	0.	0.39	0.48	0.55	0.59
TL at SCP4	0.22	0.45	0.66	1.10	1.05
Interpolated EF					
$\Delta 123$	0.38	0.44	0.48	0.56	0.58
$\Delta 1'23$	0.34	0.43	0.52	0.63	0.69
Interpolated TL					
$\Delta 123$	0.41	0.46	0.55	0.81	1.32
$\Delta 1'23$	0.38	0.49	0.70	1.10	1.84

DISCUSSION AND CONCLUSIONS

Various schemes for sounder-updating of a statistical model, MINIMUF in this case, have been tested in an analysis of data from the Solid Shield exercises. The results have shown that high MUF prediction accuracies are possible with this general approach, even with the use of a simplified statistical model. This could be part of a successful frequency management system in which N sounders are deployed in an area to obtain ionospheric data for inputs to a statistical model, e.g., MINIMUF, which predicts MUF values for various communication paths of interest. The use of oblique-incidence sounders (OIS) is not absolutely necessary; the sounder mix may include vertical-incidence sounder (VIS) assets. It will be noted, however, that the use of OIS assets could be advantageous for $N \geq 4$, since, if each site is equipped with a transmitter and receiver, it is possible to characterize the ionosphere at $N(N-1)/2$ control points. The corresponding number for VIS assets is N . Whatever the sounder mix is, the advantage of the sounder network deployment is not just to have one or another SCP in the vicinity of an ionospheric reflection point for one of various communication paths of interest. In many cases it would be possible to circumscribe a triangle of SCPs about the ionospheric reflection point and spatially interpolate the SCP data to the interior point. The procedure for this has been specified in this paper and shown to be capable of very high accuracy. For example (cf. Table 1), rms real-time MUF prediction errors are at or below 0.40 MHz with this approach, substantially more accurate than updating at any one SCP in the triangle (e.g., by more than 30% for the closest SCP).

The procedure that gives the best results here involves force-fitting the driving parameters of the statistical model (10.7 cm flux or sunspot no. in this case) to sounder MUF data, and is thus the same as previously reported in this respect. Frequent updating and the interpolation scheme have been shown to be advantageous in conjunction with this effective flux scheme, and the results also show that the scheme is best for future predictions. In this connection a particular, but not necessarily optimum, statistical forecasting scheme was tried, based on the use of trend lines for daytime forecasting. The results were not as good in this case, but a statistical forecasting scheme may yet prove to be valuable for more diffuse sounder configurations. This is currently under investigation, but the effective flux scheme certainly

does appear at this point to be most attractive for its accuracy, simplicity, and applicability to both day and night conditions.

ACKNOWLEDGMENTS

The authors would particularly like to thank P.A. Hoover for considerable efforts in processing and organization of data and assistance with computations. Timely discussions with J.M. Goodman are also appreciated. Computational assistance from E.K. Yamamura is also gratefully acknowledged.

REFERENCES

- Basler, R.P., and T.D. Scott, Ionospheric structure from oblique-backscatter soundings, Radio Sci., 8, 425-429, 1973
- Coffey, H.E., editor, Geomagnetic and solar data, World Data Center A, J. Geophys. Res., 86(A9),779, 1981
- Daehler, M., A FOT prediction procedure for HF communications frequency management, MILCOM 84 Conference Record, Paper 8.1, IEEE Military Communications Conference, Los Angeles, CA, 1984 p. 94
- Reilly, M.H. and E.K. Yamamura, Oblique ionograms and HF propagation assessment, MILCOM 84 Conference Record, Paper 8.3, IEEE Military Communications Conference, Los Angeles, CA, 1984 p. 100
- Reilly, M.H., Ionospheric true height profiles from oblique ionograms, Radio Sci., 20, 280-286, 1985a
- Reilly, M.H., Single site location with ionospheric specification from oblique-incidence sounders, NRL Memo Rpt. 5586, Washington, DC, 1985b ADA157 226
- Rose, R.B., J.N. Martin, and P.H. Levine, MINIMUMUF-3: A simplified HF MUF prediction algorithm, NOSC TR 186, San Diego, CA, 1978 ADA052052
- Rose, R.B., and J.N. Martin, MINIMUMUF-3.5, NOSC TD 201, 1978 AD-A066-256
- Sailors, D.B., W.K. Moision, and R.P. Brown, Accuracy of high frequency maximum usable frequencies (MUF) prediction, NOSC TR 695, 1981 ADA107 097
- Sailors, D.B., Tactical decision aids for HF communication, NOSC TD 782, 1984 ADB091227
- Uffelman, D.R., HF propagation assessment studies over paths in the Atlantic, NRL Memo Rpt. 4599, Washington, DC, 1981 ADA107599
- Uffelman, D.R., and L.O. Harnish, HF systems test for the SURTASS operation of February 1981, NRL Memo Rpt. 4600, 1981 ADA106 747
- Uffelman, D.R., and L.O. Harnish, Initial results from HF propagation studies during Solid Shield, NRL Memo Rpt. 4849, 1982 ADA118 492
- Uffelman, D.R., and P.A. Hoover, Real-time update of two HF channel evaluation models by oblique sounding, NRL Memo Rpt. 5246, 1984 ADA137 556
- Uffelman, D.R., L.O. Harnish, and J.M. Goodman, HF frequency management by frequency-sharing as assisted by models updated in real-time, NRL Memo Rpt. 5284, 1984 ADA139896

END

FILMED

12-85

DTIC